Redox Biology 34 (2020) 101538

Contents lists available at ScienceDirect

Redox Biology

journal homepage: www.elsevier.com/locate/redox

SIRT1 agonism modulates cardiac NLRP3 inflammasome through pyruvate dehydrogenase during ischemia and reperfusion

Ying Han[a,b,1], Weiju Sun[b,c,1], Di Ren[b], Jingwen Zhang[b], Zhibin He[b], Julia Fedorova[b], Xiaodong Sun[d], Fang Han[d], Ji Li[b,*]

[a] Cardiovascular Department, The Fourth Affiliated Hospital of Harbin Medical University, Harbin, 150001, China
[b] Department of Surgery, University of South Florida, Tampa, USA
[c] Cardiovascular Department, The First Affiliated Hospital of Harbin Medical University, Harbin, 150001, China
[d] Department of Physiology and Biophysics, Mississippi Center for Heart Research, University of Mississippi Medical Center, Jackson, USA

ARTICLE INFO

Keywords:
SIRT1 agonist
NLRP3 inflammasome
ROS
Ischemia/reperfusion

ABSTRACT

Nucleotide-binding oligomerization domain-Like Receptor with a Pyrin domain 3 (NLRP3) inflammasome was emerged as a marker of metabolic dysregulation. We revealed that age-related Sirtuin-1 (SIRT1) modulates cardiac metabolism that medicated inflammatory response during ischemia and reperfusion (I/R) stress. We hypothesize that SIRT1 attenuates NLRP3 inflammasome-dependent inflammation and pyroptosis during myocardial I/R through metabolic modulation. C57BL/6J wild type (WT) mice, inducible cardiomyocyte specific SIRT1 knockout (icSIRT1 KO) and inducible cardiomyocyte specific PDH E1α knockout (icPDH E1α KO) mice were subjected to ligation and release of left anterior descending coronary artery for *in vivo* regional I/R models. The echocardiography measurement demonstrated that SIRT1 agonist SRT1720 (30 μg/g) improved cardiac systolic function during 45 min of ischemia and 6 h of reperfusion in C57BL/6J WT mice. The biochemical analysis showed that I/R triggered activation of cardiac pyruvate dehydrogenase (PDH), while SIRT1 agonist SRT1720 inhibited I/R-induced PDH activity and reduced production of reactive oxygen species (ROS) during myocardial I/R. Moreover, SRT1720 regulates PDH-related glucose oxidative metabolism to reduce NLRP3 inflammasome activation and pyroptosis in an Akt signaling dependent manner during I/R. Furthermore, an impaired Akt signaling was observed in icSIRT1 KO versus $SIRT1^{flox/flox}$ mice under I/R stress. Intriguingly, we observed lower levels of ROS generation, decreased NLRP3 levels and less pyroptosis occurred in the icPDH E1α KO versus PDH $E1\alpha^{flox/flox}$ hearts during I/R. Taken together, the results indicate that SIRT1 agonism can inhibit activation of NLRP3 inflammasome via Akt-dependent metabolic regulation during ischemic insults by I/R.

1. Introduction

Acute myocardial infarction (AMI) remains the leading cause of morbidity and mortality worldwide [1], despite the treatments of considerable improvements, such as primary percutaneous coronary interventions that provide early and successful myocardial reperfusion [2,3]. However, the process of rapid restoration of blood flow to myocardium (reperfusion) can lead to paradoxical cardiomyocyte dysfunction and worsen tissue damage known as “ischemia/reperfusion (I/R) injury” [3–10]. The exact mechanisms of I/R injury are not fully known [11]. Sterile inflammation is considered to be one of paramount importance for I/R injury development [12,13].

Emerging evidence indicates the role of inflammasome as one of the key regulators of this inflammation-mediated I/R injury [14]. The inflammasome is a multiprotein complex that embodies caspase-1, apoptosis-associated speck-like protein (ASC), and nucleotide-binding oligomerization domain-like receptor with a pyrin domain (NLRP) [15]. Assembly of an inflammasome triggers proteolytic cleavage of dormant procaspase-1 into active caspase-1, which converts the cytokine precursors pro-interleukin-1β (IL-1β) and pro-interleukin-18 (IL-18) into mature and biologically active IL-1β and IL-18, respectively [16,17]. Mature IL-1β is a potent proinflammatory mediator in many immune reactions, including the recruitment of innate immune cells to the site of infection and modulation of adaptive immune cells, whereas mature

* Corresponding author. Department of Surgery, Morsani College of Medicine, University of South Florida, 12901 Bruce B. Downs Blvd, MDC 110, Tampa, FL, 33612, USA.
E-mail address: jili@usf.edu (J. Li).
[1] These authors contributed equally to this work.

https://doi.org/10.1016/j.redox.2020.101538
Received 26 February 2020; Received in revised form 30 March 2020; Accepted 7 April 2020
Available online 13 April 2020

IL-18 is important for the production of interferon-γ and potentiation of cytolytic activity of natural killer cells and T cells [18]. Active caspase-1 also induces a proinflammatory form of cell death, known as pyroptosis [19]. Among the inflammasomes, NLRP3 inflammasome is the most studied inflammasome and been known as a decisive component of the innate immune response to ischemia, repair, and perpetuation of injury [20–22].

NLRP3 inflammasome assembly is strictly regulated by the requirement of coordinated priming and activation signals. These signals are highly diverse, and despite almost 20 years of research, our understanding of the signaling pathways and the molecular mechanisms controlling NLRP3 remains largely incomplete. Metabolic regulation of NLRP3 and other inflammasome components have recently emerged as an important mechanism [23]. The NLRP3 inflammasome has been shown to sense metabolites such as palmitate [24], uric acid [25], and cholesterol crystals [23], and is inhibited by ketone bodies [26] produced during metabolic flux. The NLRP3 inflammasome has also been shown to be regulated by mitochondrial reactive oxygen species (ROS) and components of glycolysis, such as Hexokinase [27,28].

Sirtuin-1 (SIRT1), a member of the NAD-dependent sirtuin family of histone/protein deacetylases (HDAC), has emerged as a critical regulator during I/R in the heart, as well as in aged heart identified by our previous work [29–33]. It plays an important role in inhibiting apoptosis, protecting mitochondrial function, resisting oxidative stress and

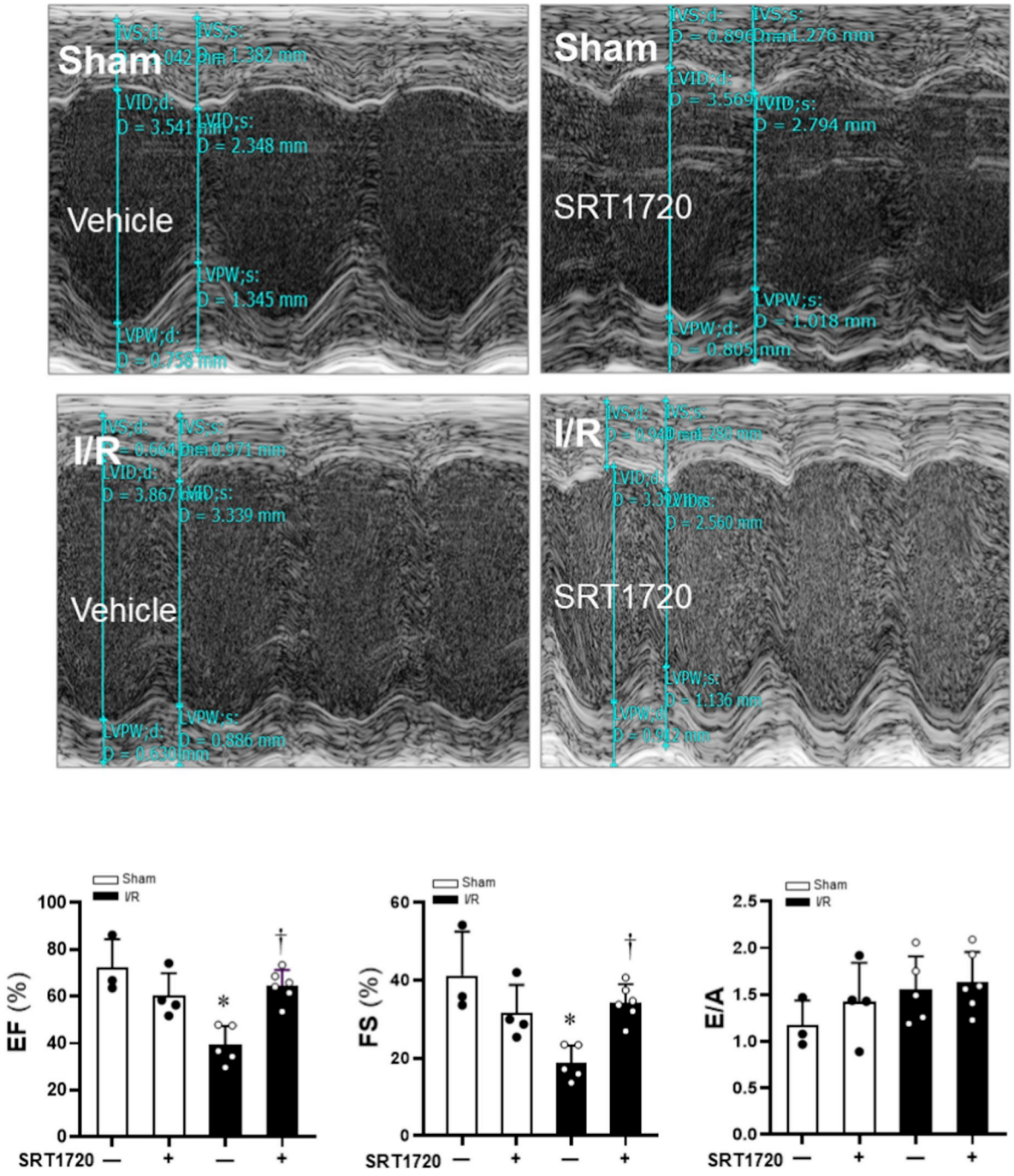

Fig. 1. Effects of SIRT1 agonist SRT1720 on cardiac function of C57BL/6J under sham operations and ischemia and reperfusion stress conditions. Echocardiography measurements to determine the effects of SRT1720 treatments on contractile functions of mouse hearts under physiological and pathological conditions. N = 3–6, data are mean ± standard error, *$p < 0.05$ *vs.* Sham with vehicle; †$p < 0.05$ *vs.* I/R with vehicle.

alleviating inflammatory reaction, including the inhibition of the NLRP3 inflammsome. SIRT1 was reported to exhibit a role in NLRP3 inflammasome modulation and SIRT1 KO mice have increased levels of active IL-1β in the lungs in a model of sepsis [34]. In endothelial cells SIRT1 knockdown enhanced NLRP3 inflammasome activation and SIRT1 stimulation inhibited NLRP3 inflammasome activation [35]. Resveratrol also can alleviate cerebral ischemia/reperfusion injury in rats by inhibiting NLRP3 inflammasome activation through SIRT1-dependent autophagy induction [36]. However, the molecular mechanisms remain elusive. Here we revealed a critical role of SIRT1's metabolic regulation in NLRP3 inflammasome-dependent inflammation and pyroptosis in response to I/R stress.

2. Materials and methods

2.1. Experimental animals

C57BL/6 J wild type mice (4–6months), SIRT1$^{flox/flox}$ mice (stock number 008041), and CreER^{T2} (stock number 005657) mice were from Jackson Laboratory. Cardiomyocyte specific deletion of the SIRT1 gene mouse was generated by breeding SIRT1$^{flox/flox}$ mice with transgenic mice that carried an autosomally integrated Cre gene driven by the cardiac-specific alpha-myosin heavy chain promoter (αMHC) (CreER^{T2}). The inducible cardiac-specific SIRT1 knockout (icSIRT1 KO) mice were generated by Tamoxifen injection (0.04 mg/g, i.p. 5 days) of CreER^{T2}-SIRT1$^{flox/flox}$ (12 weeks old) mice, and SIRT1$^{flox/flox}$ mice (12 weeks old) with Tamoxifen injection were used for control groups. Cardiac-specific deletion of the PDHa1 gene was also generated by breeding PDH E1α$^{flox/flox}$ mice [37] with transgenic mice that carried an autosomally integrated Cre gene driven by the cardiac-specific aMHC (CreER^{T2}). The inducible cardiac-specific PDH E1α knockout (icPDH E1α KO) mice were generated by Tamoxifen injection (0.04 mg/g, ip 5 days), and PDH E1α$^{flox/flox}$ (12 weeks old) mice with Tamoxifen injection were used for control groups. The genotying details were described in the Supplementary material online. All animal experiments were performed in compliance with NIH guidelines. And All animal protocols in this study were approved by the University of South Florida Institutional Animal Care and Use Committee.

2.2. In vivo regional I/R model

Mice were anesthetized with isoflurane (2%) *via* inhalation and kept ventilated (Harvard Rodent Ventilator; Harvard Apparatus, Holliston, MA) during surgeries. The body temperature was maintained at 37 ˚C with a heating pad. After left lateral thoracotomy, the left anterior descending coronary artery (LAD) was occluded 45 min for ischemia with an 8-0 nylon suture and polyethylene tubing to prevent arterial injury. An ECG and blanching of the left ventricle confirmed ischemic repolarization changes (ST-segment elevation) during coronary occlusion. Meanwhile, mice were injected with SIRT1 agonist SRT1720 (30 μg/g, i.p.) or vehicle (DMSO) before surgery. Hemodynamic parameters were detected at 6 h at the end of reperfusion. At the endpoints of experiments, mice were anesthetized with isoflurane (2%) and ventilated while the hearts were excised, and the ischemic region of the left ventricle was separated before freeze clamping in liquid nitrogen. Freeze clamped heart tissues were stored at -80 ˚C until further immunoblotting analysis.

2.3. Echocardiography

Transthoracic echocardiography was performed on mice at rest, following anesthesia with 1.5%–2.0% isoflurane, using a high-resolution imaging system for small animals (a Vevo 3100 imaging system, Visual Sonics). All hair was removed from the chest with a chemical hair remover. Parasternal long-axis and short-axis views were acquired. The left ventricular (LV) dimensions and wall thicknesses were determined from parasternal short axis M-mode images.

2.4. Histopathological analysis

To assess the morphological changes, the LV tissues were fixed immediately in 10% neutral buffered formalin and embedded in paraffin after anesthesia. Then the sections (5 μm) cut from the paraffin blocks were stained with haematoxylin-eosin for histopathological examination.

2.5. TUNEL fluorescent assay and mitochondrial reactive oxygen species (ROS) measurement

TUNEL fluorescent assay was conducted with an *in-situ* Cell Death Detection Kit (Roche Inc., Indianapolis, IN, United States) following the protocols using freshly frozen sections of LV. Sections were counterstained by DAPI (1:1000) for 5 min. The sections were then washed with PBS three times and covered by microscopic glass with Antifade Mounting Medium (Beyotime Institute of Biotechnology, Shanghai, China) for further study. The numbers of TUNEL-positive cells in the hippocampal CA1 region were counted and analyzed (at × 200 and ×400 magnification) by an investigator blinded to the treatment conditions.

Mitochondrial ROS production was evaluated by MitoSOX Red (Invitrogen). Freshly frozen sections of LV were washed by PBS and then incubated with in PBS containing 1 μM MitoSOX™ Red mitochondrial superoxide indicator (Invitrogen) for 10 min at 37 ˚C, protected from light. Images were detected by fluorescence microscopes (excitation at 510, emission at 580 nm).

Table 1
Other echocardiographic assessment of cardiac functions.

Parameter (unit)	Sham		I/R	
	Vehicle	SRT1720	Vehicle	SRT1720
IVSd (mm)	0.90 ± 0.23	0.99 ± 0.14	0.64 ± 0.06*	0.82 ± 0.27†
IVSs (mm)	1.26 ± 0.44	1.24 ± 0.18	0.70 ± 0.19*	0.98 ± 0.35
LVIDd (mm)	3.28 ± 0.23	3.30 ± 0.24	3.68 ± 0.14*	3.16 ± 0.37
LVIDs (mm)	1.94 ± 0.47	2.26 ± 0.23	2.99 ± 0.22*	2.09 ± 0.35†
LVPWd (mm)	0.86 ± 0.24	0.93 ± 0.23	0.71 ± 0.19	0.95 ± 0.49
LVPWs (mm)	1.42 ± 0.34	1.29 ± 0.30	0.90 ± 0.21	1.34 ± 0.34
LV Vol; d (mm)	43.69 ± 7.62	44.53 ± 7.75	57.36 ± 5.14*	40.53 ± 11.05†
LV Vol; s (mm)	12.63 ± 6.97	17.50 ± 4.48	34.91 ± 6.40*	14.80 ± 6.12†
LV mass (mm)	98.64 ± 31.65	111.71 ± 6.31	82.54 ± 20.03	95.98 ± 39.78

Abbreviations: IVSd: interventricular septal end diastole, IVSs: interventricular septal end sistole, LVIDd: left ventricular internal diameter end diastole, LVIDs: left ventricular internal diameter end sistole, LVPWd: left ventricular posterior wall end diastole, LVPWs: left ventricular posterior wall end sisstole. Values are means ± standard error. *$p < 0.05$ *vs.* Sham with Vehicle; †$p < 0.05$ *vs.* I/R with Vehicle.

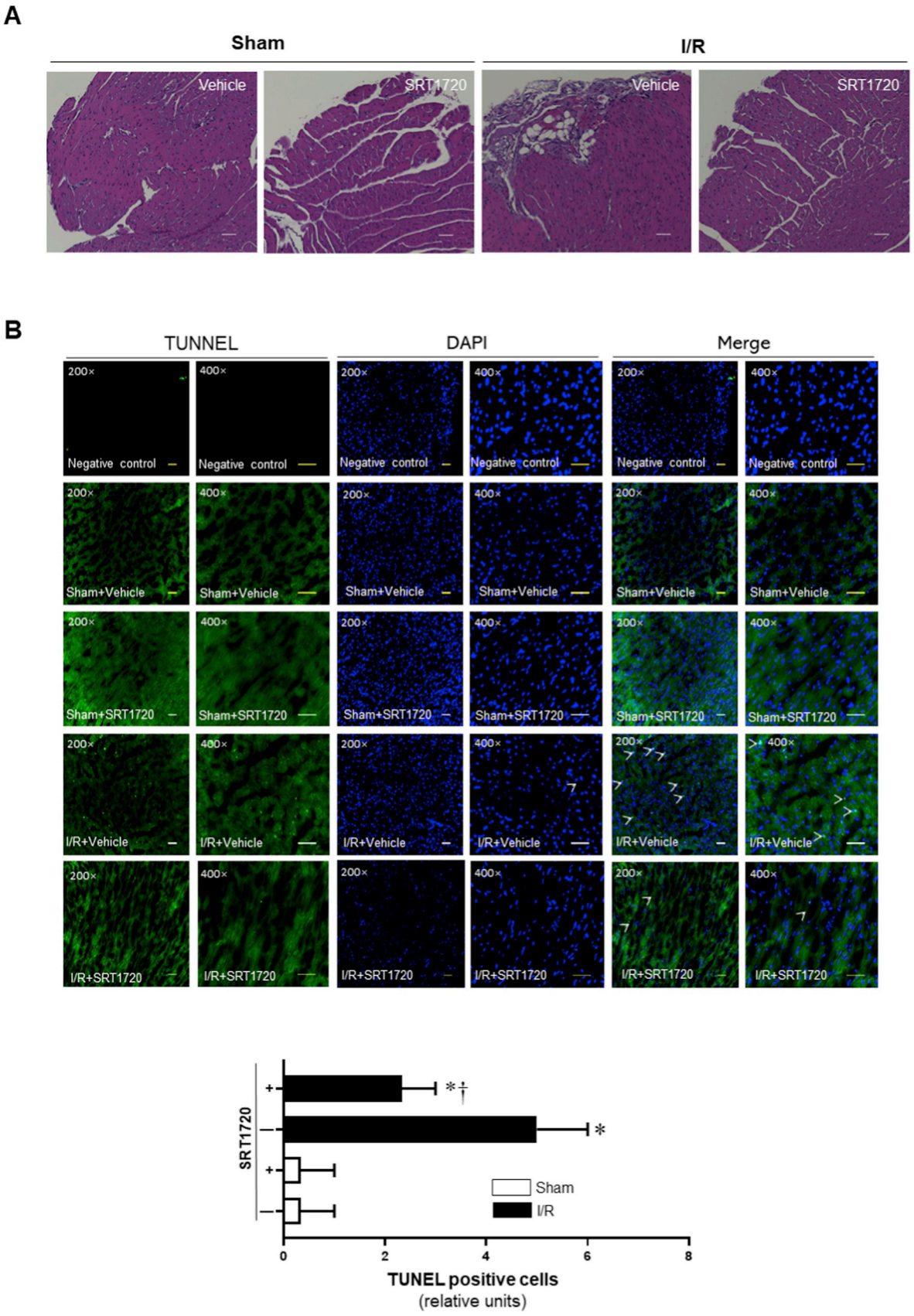

Fig. 2. Effects of SRT1720 treatments on histopathological damage and pyroptosis caused by 45 min of ischemia and 6 h of reperfusion (I/R). (A) Representative images of haematoxylin and eosin staining for sham operations and I/R with or without SRT1720 treatments. (B) Upper: representative TUNEL staining for myocardial tissue from sham operations and I/R with or without SRT1720 treatments; Lower: bar graph of quantitative analysis for TUNEL positive cells from sham operations and I/R with or without SRT1720 treatments, n = 3–5 independent experiments, data are mean ± standard error, $^{*}p < 0.05$ *vs.* Sham with vehicle, respectively; †$p < 0.05$ *vs.* I/R with vehicle.

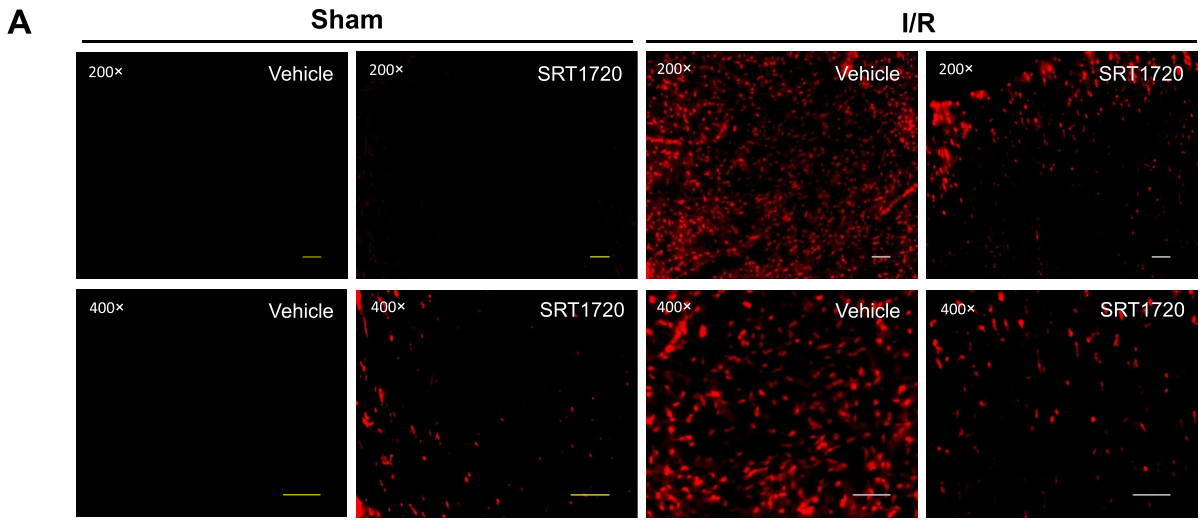

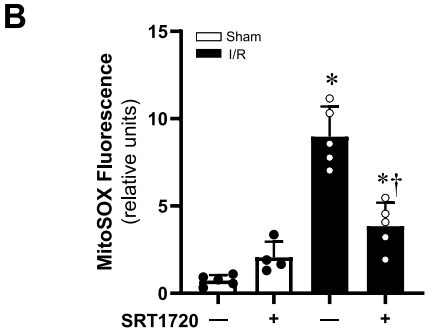

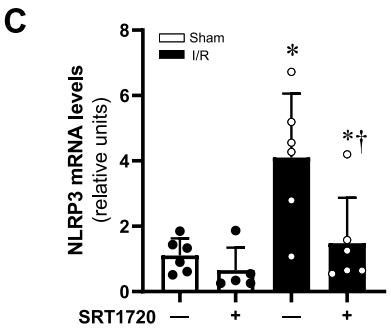

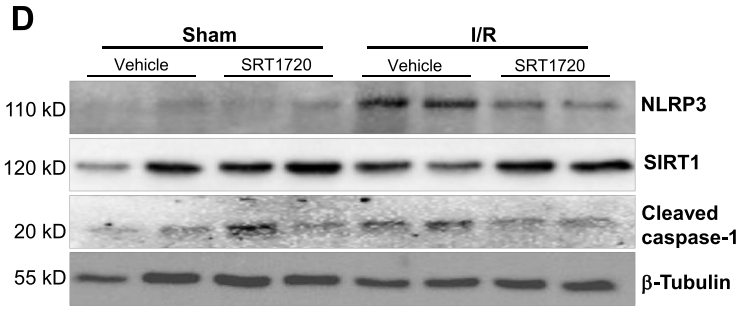

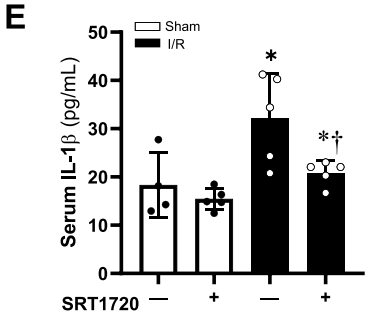

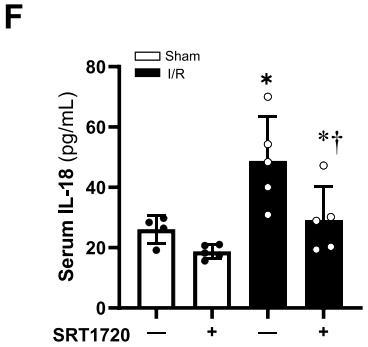

(caption on next page)

Fig. 3. Association of reactive oxygen species (ROS) with NLRP3 inflammasome activation during ischemia and reperfusion (I/R) stress. (A) Representative images of mitochondrial superoxide production (MitoSOX, red fluorescence). (B) Quantitative analysis of MitoSOX production. n = 5, $*p < 0.05$ *vs.* Sham, respectively; $\dagger p < 0.05$ *vs.* I/R alone. (C) Real-time RT-PCR to measure NLRP3 mRNA expression levels. n = 5, $*p < 0.05$ *vs.* Sham with vehicle, respectively; $\dagger p < 0.05$ *vs.* I/R with vehicle. (D) Upper: the immunoblotting to show the protein levels of cardiac NLRP3 under sham operations and I/R with or without SRT1720 treatments; Lower: quantitative analysis of NLRP3 and SIRT1 protein levels under sham and I/R with or without SRT1720 treatments. n = 5–6/group, $*p < 0.05$ *vs.* Sham with vehicle, respectively; $\dagger p < 0.05$ *vs.* I/R with vehicle. (E) The serum IL-1β levels with ELISA Kit determination for Sham and I/R with or without SRT1720 treatments. n = 4–5/group, $*p < 0.05$ *vs.* Sham with vehicle, respectively; $\dagger p < 0.05$ *vs.* I/R with vehicle. (F) The serum IL-18 levels with ELISA Kit determination for Sham and I/R with or without SRT1720 treatment. n = 4–5/group, $*p < 0.05$ *vs.* Sham with vehicle, respectively; $\dagger p < 0.05$ *vs.* I/R with vehicle. (For interpretation of the references to colour in this figure legend, the reader is referred to the Web version of this article.)

2.6. Immunoblotting

Protein samples were prepared from hearts using lysis buffer (20 mM Tris-HCl [pH 7.5], 137 mM NaCl, 0.5% NP-40, 0.5 mM 1,4-Dithiothreitol (DTT), Complete Protease Inhibitor Cocktail [Roche, Mannheim, Germany], and Phosphatase Inhibitor Cocktail [Sigma]). Immunoblots and immunoprecipitations were performed as previously described [38,39]. Protein concentrations were measured using a Bradford assay kit (Bio-Rad, Hercules, CA). The proteins were separated by 7–15% SDS-PAGE and then transferred to nitrocellulose membranes (Bio-Rad). The membranes were incubated with primary antibodies against NLRP3, AMP-activated protein kinase (AMPK), phosphor-AMPK (Thr^{172}), pyruvate dehydrogenase (PDH), phosphor-PDH (Ser^{293}), Acetyl CoA Carboxylase (ACC), phosphor-ACC (Ser^{79}), Phosphatidylinositol-4,5- bisphosphate 3-kinase (PI3K), phosphor-PI3K p85 (Tyr^{458})/p55 (Tyr^{199}), protein kinase B (Akt), phosphor-Akt (Ser^{473}), phosphatase and tensin homologue deleted on chromosome ten (PTEN) phosphor-PTEN (Ser^{380}) and Carnitine palmitoyltransferase-1 (CPT1) (obtained from Cell Signaling, Danvers, MA). Mice SIRT1 antibody was obtained from Abcam (MitoSciences-Abcam, Eugene, OR). Horseradish peroxidase-conjugated secondary antibodies were obtained from Cell Signaling.

2.7. Real-time qPCR analysis

Total RNA from LV myocardial tissues was extracted using Trizol (Invitrogen, USA) and then synthesized into cDNA by using an Applied Biosystems™ TaqMan™ High-Capacity RNA-to-cDNA Kit (Applied Biosystems, USA, #4387406). qPCR was performed using iTaq Universal SYBR Green Supermix (Bio-Rad, #1725124). Primer sequences were listed in the supplementary materials.

2.8. Enzyme-linked immunosorbent assay

Blood samples (0.2 ml) were extracted at the endpoints of experiments and injected into EDTA anticoagulant tubes and maintained at 4 °C for 30 min, followed by centrifugation at 3000 × *g* for 10 min at 4 °C to collect supernatant. The quantifications of IL-1β (cat. no. ab197742) and IL-18 (cat. no. ab216165; both Abcam, Cambridge, UK) in serum of different groups were performed using an enzyme-linked immunosorbent assay (ELISA) kit following the manufacturer's protocols.

2.9. Statistical analysis

Data were collected from experimental animals (n = 3–7 per group) and presented as means ± SEM, as indicated, using Image GraphPad Prism 8.0 software (GraphPad Software, La Jolla, CA) for analysis. Comparisons were performed using either a two-tailed, unpaired Student's *t*-test or ANOVA using Tukey's posttest. A value of $p < 0.05$ was considered statistically significant.

3. Results

3.1. SIRT1 agonist improves cardiac systolic function under I/R

Echocardiographic measurements of ejection fraction (EF), fractional shortening (FS), the ratio of peak velocity blood flow from left ventricular relaxation in early diastole (the E wave) to peak velocity flow in late diastole caused by atrial contraction (the A wave) (E/A ratio) were shown in Fig. 1. Other Parameters including interventricular septal (IVS) dimensions, LV internal dimensions (LVID), LV posterior wall thickness (LVPW) and LV mass in C57BL/6J mice were shown in Table 1. The results demonstrated that the systolic functions were significantly impaired during 45 min of ischemia and 6 h of reperfusion (I/R) as shown by reduced EF and FS (Fig. 1). SIRT1 agonist SRT1720 treatments significantly improved cardiac systolic function during 45 min of ischemia and 6 h of reperfusion as compared to the I/R group (Fig. 1). However, the cardiac diastolic functions were not affected by 45 min of ischemia and 6 h of reperfusion or SRT1 agonist treatment (Fig. 1).

3.2. SRT1720 attenuates histopathological damage and cardiac pyroptosis caused by ischemia and reperfusion

The HE immunohistochemistry results showed that the pathological features of myocardial destruction became apparent during 6 h of reperfusion after 45 min of ischemia in heart tissue with deformation of myocardial fibers, swelling and rupture of myocardial cells, obvious infiltration of inflammatory cells (Fig. 2A). However, SIRT1 agonist SRT1720 treatment ameliorated the histological features that became typical of normal cardiac structure or mild architectural damage, characterized by interstitial edema and localized necrotic areas (Fig. 2A).

The TUNEL fluorescent assay showed that ischemia (45 min) and reperfusion (6 h) caused the higher percentage of dead cardiomyocytes than that in the control groups (Fig. 2B). Interestingly, SRT1720 treatment reduced the pyroptotic cell death induced by I/R injury (Fig. 2B). These results suggest that SIRT1 activation by SRT1720 can ameliorates cardiac pyroptosis caused by ischemia and reperfusion injury.

3.3. SIRT1 activation inhibits ROS-associated NLRP3 inflammasome activation

Since ROS accumulation is a well-established mechanism of NLRP3 inflammasome activation and mitochondrial ROS is the main source of ROS during myocardial ischemia and reperfusion injury, we determined the ROS levels in the heart during sham operations or 45 min of ischemia and 6 h of reperfusion with an approach of a fluorescent probe (MitoSOX Red). The results demonstrated that the ROS levels were dramatically increased during myocardial I/R versus sham operation groups (Fig. 3A–B). SIRT1 agonist SRT1720 significantly reduced ROS production caused by I/R (Fig. 3A–B). Intriguingly, I/R can trigger both mRNA and protein expression of the NLRP3 inflammasome while

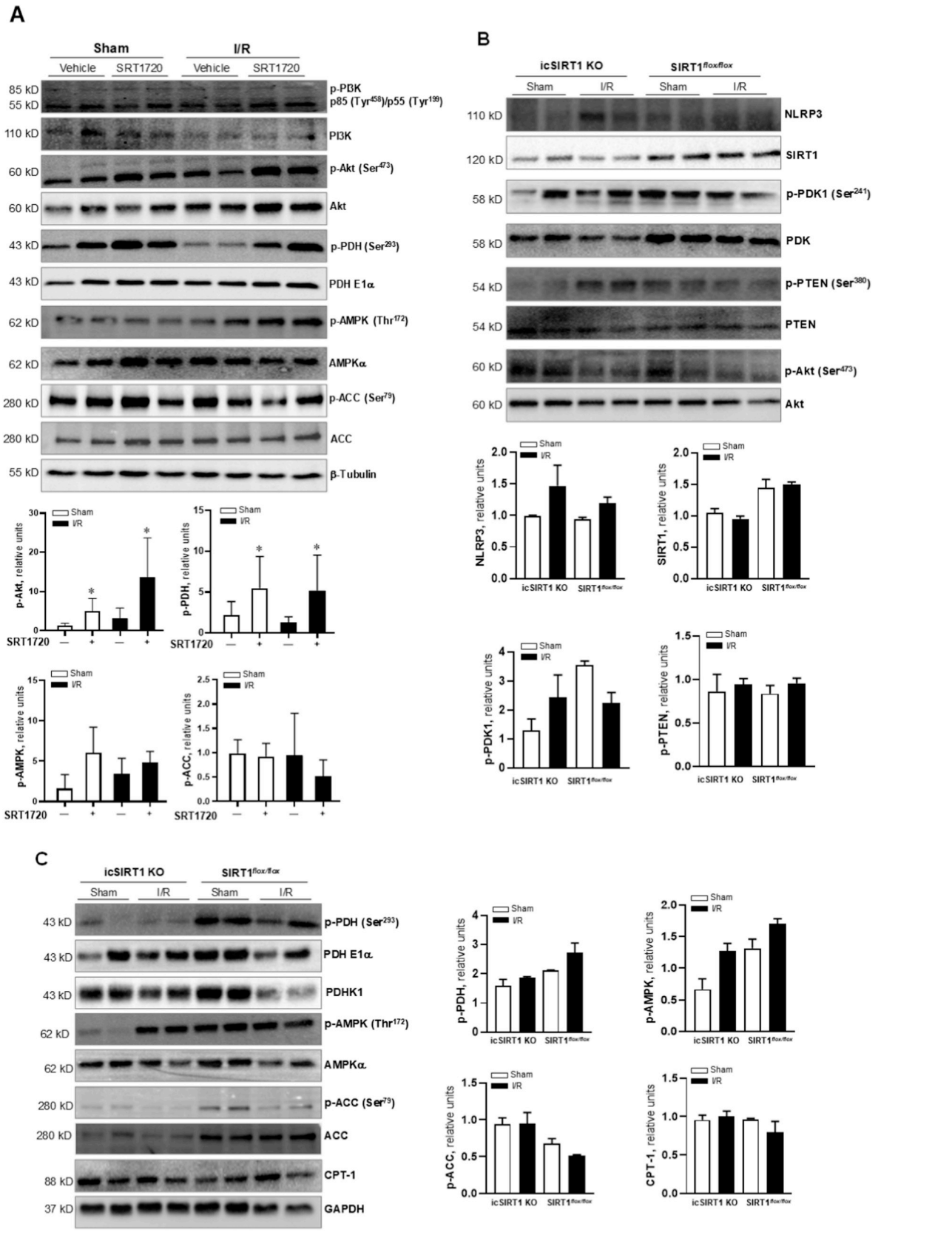

Fig. 4. Effects of SIRT1 agonist SRT1720 on Akt signaling mediated pyruvate dehydrogenase (PDH) activation. (A) Left: the immunoblotting to show PI3K, Akt, PDH, AMPK and ACC signaling response in the heart under sham and I/R with or without SRT1720 treatments. Right: quantitative analysis of Akt, PDH, AMPK signaling pathways in the heart under sham and I/R with or without SRT1720 treatments. n = 4–6 mice/each group, $*p < 0.05$ *vs.* Sham with vehicle or I/R with vehicle, respectively. (B) The immunoblotting for NLRP3, SIRT1, PDK1, PTEN and Akt signaling response in icSIRT1 KO and SIRT1$^{flox/flox}$ hearts under sham or I/R conditions. (C) The immunoblotting for PDH, AMPK, and CPT-1 signaling response in icSIRT1 KO and SIRT1$^{flox/flox}$ hearts under sham or I/R conditions.

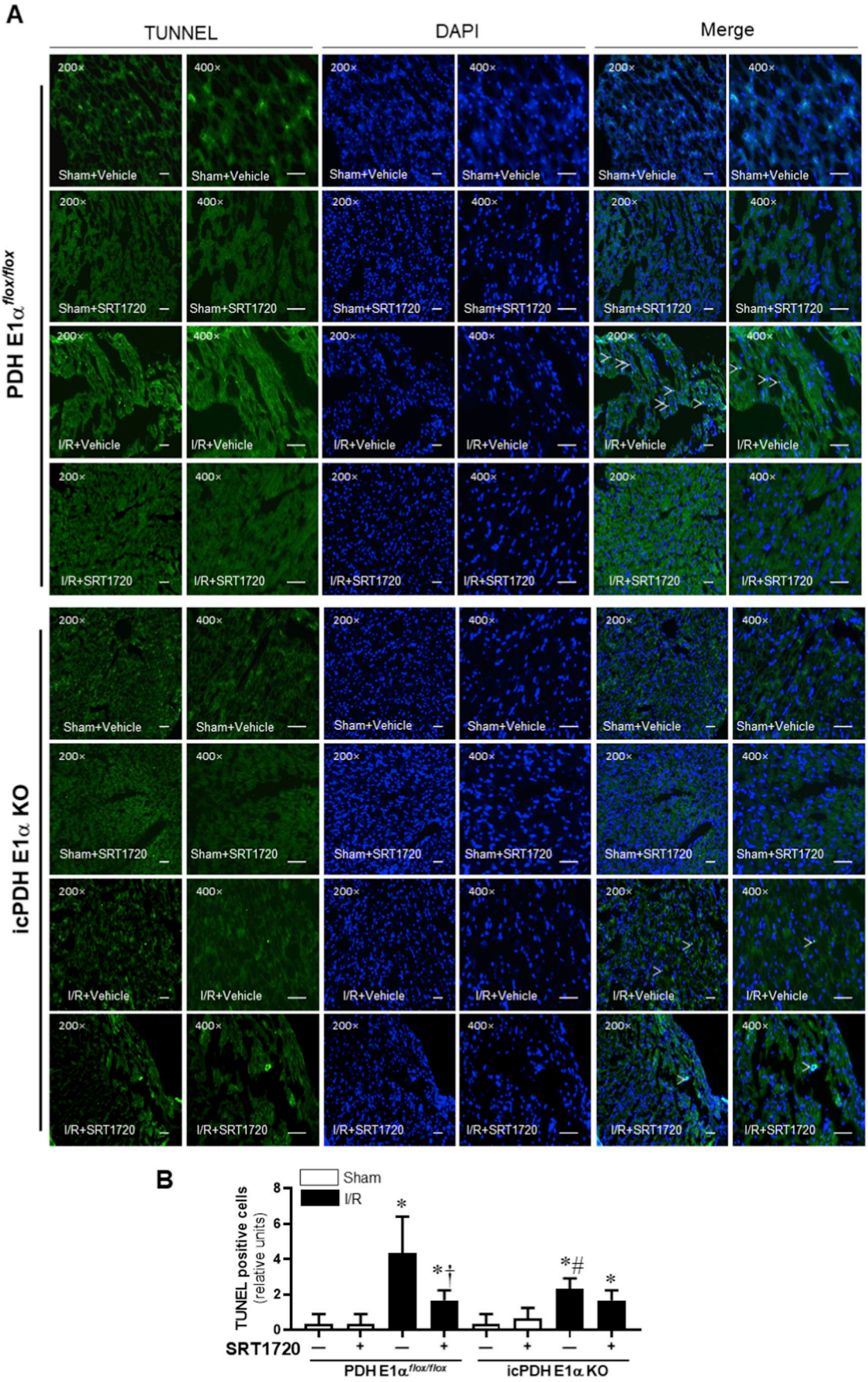

(caption on next page)

Fig. 5. Effects of SIRT1 agonist SRT1720 on cardiomyocytes pyroptosis in PDH E1α$^{flox/flox}$ and icPDH E1α KO mice under sham operations and I/R with or without SRT1720 treatments. (A) The representative TUNEL staining of myocardial tissue from PDH E1α$^{flox/flox}$ and icPDH E1α KO mice under sham operations and I/R with or without SRT1720 treatments. (B) bar graph of quantitative analysis for TUNEL positive cells from sham operations and I/R with or without SRT1720 treatments in PDH E1α$^{flox/flox}$ and icPDH E1α KO mice, n = 3–5 independent experiments, data are mean ± standard error, *$p < 0.05$ *vs.* Sham, respectively; †$p < 0.05$ *vs.* I/R with vehicle in PDH E1α$^{flox/flox}$; #$p < 0.05$ *vs.* I/R with vehicle in PDH E1α$^{flox/flox}$.

SRT1720 treatment significantly reduced NLRP3 inflammasome at both mRNA and protein levels although the SIRT1 protein levels did not change under these conditions (Fig. 3C–D). The downstream effectors of NLRP3 inflammasome serum IL-1β and IL-18 levels were significantly increased in response to I/R stress and the administration of SRT1720 reduced both serum IL-1β and IL-18 levels caused by I/R stress (Fig. 3E–F).

3.4. SIRT1 agonist modulates cardiac Akt-PDH signaling cascade

The production of ROS is associated with aerobic respiration. Decarboxylation of acetyl-CoA in mitochondria by PDH links glycolysis to the Krebs cycle and controls the rate of aerobic respiration. Therefore, we determined whether SIRT1 agonist SRT1720 treatment can attenuate myocardial abnormality *via* modulating PDH activity through metabolic reprogramming. The immunoblotting results demonstrated that SRT1720 treatment significantly enhanced phosphorylation of PDH that reflects a reduced PDH activity (Fig. 4A). Intriguingly, SRT1720 treatment triggered phosphorylation of Akt that has been implicated in modulating cardiac metabolism (Fig. 4A). But the phosphorylation of PI3K did not affected by SRT1720 treatment (Fig. 4A). The SIRT1 agonist SRT1720 did not trigger energy sensor AMPK signaling pathway, as shown by the immunoblotting with phosphorylation of AMPK and downstream ACC (Fig. 4A). To further determine the role of SIRT1 in the Akt-PDH signaling pathway, icSIRT1 KO versus SIRT1$^{flox/flox}$ mice were subjected to 45 min of ischemia and 6 h of reperfusion or sham operations. The immunoblotting data showed that icSIRT1 KO versus SIRT1$^{flox/flox}$ hearts had higher NLRP3 levels and phosphorylation of PTEN in response to I/R stress (Fig. 4B). icSIRT1 KO blunted phosphorylation of PDH and AMPK signaling pathway as shown by phosphorylation of AMPK and downstream ACC versus SIRT1$^{flox/flox}$ mouse hearts (Fig. 4C).

3.5. Cardiomyocyte specific PDH E1α deficiency blunts the effect of SIRT1 agonist on cardiac pyroptosis during I/R injury

We generated icPDH E1α KO mice with PDH E1α$^{flox/flox}$ mice to determine the role of activation of PDH in the effect of SIRT1 agonism on pyroptosis induced by I/R. The TUNEL staining results demonstrated that 45 min of ischemia and 6 h of reperfusion caused pyroptosis in the heart (Fig. 5A–B) and PDH E1α deletion in cardiomyocytes (icPDH E1α KO) had more pyroptosis occurred in the heart than that in PDH E1α$^{flox/flox}$ heart (Fig. 5A–B). Interestingly, SIRT1 agonist SRT1720 treatment significantly reduced the pyroptosis induced by I/R in PDH E1α$^{flox/flox}$ hearts (Fig. 5A) but not in icPDH E1α KO hearts (Fig. 5B). These results indicated that PDH plays a critical role in mediating the beneficial effect of SRT1720 on cardiac pyroptosis induced by ischemia and reperfusion injury.

3.6. Pyruvate dehydrogenase plays a role in I/R-triggered ROS and activation of NLRP3 inflammasome in the heart

The MitoSOX staining results showed that I/R dramatically triggered ROS generations in the hearts and the ROS levels in PDH E1α$^{flox/flox}$ hearts caused by I/R were significantly higher than that in icPDH E1α KO hearts (Fig. 6A–B). SIRT1 agonist SRT1720 can significantly reduce I/R-induced ROS in PDH E1α$^{flox/flox}$ hearts but not in icPDH E1α KO hearts (Fig. 6A–B). Moreover, administration of SRT1720 significantly deceased the protein levels of cardiac NLRP3 and downstream serum IL-1β and IL-18 concentrations in PDH E1α$^{flox/flox}$ mice (Fig. 6C–E). Interestingly, icPDH E1α KO versus PDH E1α$^{flox/flox}$ demonstrated lower ROS levels and lower levels of NLRP3 under both sham operations and I/R conditions (Fig. 6A–E). However, SRT1720 significantly reduced ROS production and NLRP3 levels caused by I/R in PDH E1α$^{flox/flox}$ hearts but not in icPDH E1α KO hearts (Fig. 6A–E). The NLRP3 downstream effectors serum IL-1β and IL-18 were significantly up-regulated by I/R in PDH E1α$^{flox/flox}$ but not in icPDH E1α KO mice (Fig. 6C–D). SIRT1 agonist SRT1720 treatments reduced both serum IL-1β and IL-18 levels in PDH E1α$^{flox/flox}$ mice (Fig. 6C–D). Interestingly, icPDH E1αKO versus PDH E1α$^{flox/flox}$ hearts showed trend of lower AMPK activation and higher levels of CPT-1 (Fig. 6E).

4. Discussion

The present study verified the molecular mechanism of SIRT1 on NLRP3 inflammasome activation in response to myocardial I/R stress. SIRT1 activation inhibited ROS-associated NLRP3 inflammasome activation and ameliorates cardiac pyroptosis during myocardial I/R injury through Akt- PDH signaling pathway. To the best of our knowledge, it for the first time identified the critical mechanism of SIRT1 regulating NLRP3 inflammasome dependent inflammation and pyroptosis against myocardial I/R injury through metabolic reprogramming.

AMI represents a prototypical example of sterile injury, in which the NLRP3 inflammasome coordinates an inflammatory response in the absence of pathogens [40]. Although the inflammatory response is needed to coordinate the clearance of cellular debris, it leads to continual loss of functional cardiomyocytes, deleterious structural abnormalities and aneurysm formation, further exacerbating the consequences injury even after reperfusion [41–43]. NLRP3 is mainly expressed in fibroblast and endothelial cells, but also in cardiomyocytes [20,44,45]. We found that NLRP3 expression levels significantly increased at 6 h of reperfusion after ischemia, that was consistent with the previous study [14]. The NLRP3 inflammasome is a critical component of inflammasomes that regulates the cleavage of caspase-1, which controls the processing and secretion of the pro-inflammatory cytokines IL-1β and IL-18. These cytokines are crucial in initiating or amplifying the innate immune response, resulting in a novel inflammatory form of programmed cell death deemed pyroptosis [46–48]. This study provided evidence that the elevated serum IL-1β and IL-18 levels and cardiomyocyte pyroptosis occurred in parallel with the impaired cardiac systolic function during I/R injury.

Recent evidence supports a role for metabolic reprogramming in NLRP3 activation and dysregulation. The discovery of an altered metabolism in activated macrophages and associated metabolic components which can drive inflammation hold much promise in unraveling a bioenergetics-independent role of metabolism in host survival [49]. It is well known that cardiac fatty acid and glucose metabolism, specifically fatty acid β-oxidation and glucose oxidation, are highly regulated processes that meet most myocardial energetic requirements. Cardiac ischemia and reperfusion are characterized by complex alterations in fatty acid and glucose oxidation that ultimately have a negative impact on cardiac efficiency and function. Such alterations in energy substrate metabolism can limit the deficits in cardiac efficiency and function that occur during cardiac ischemia and reperfusion [50]. As an important cardiac energy metabolism regulator, it leads to the hypothesis that SIRT1 can regulate NLRP3 inflammation activation through metabolic reprogramming. Since the control of PDH activity is an essential part of the overall control of glucose metabolism, we found significantly

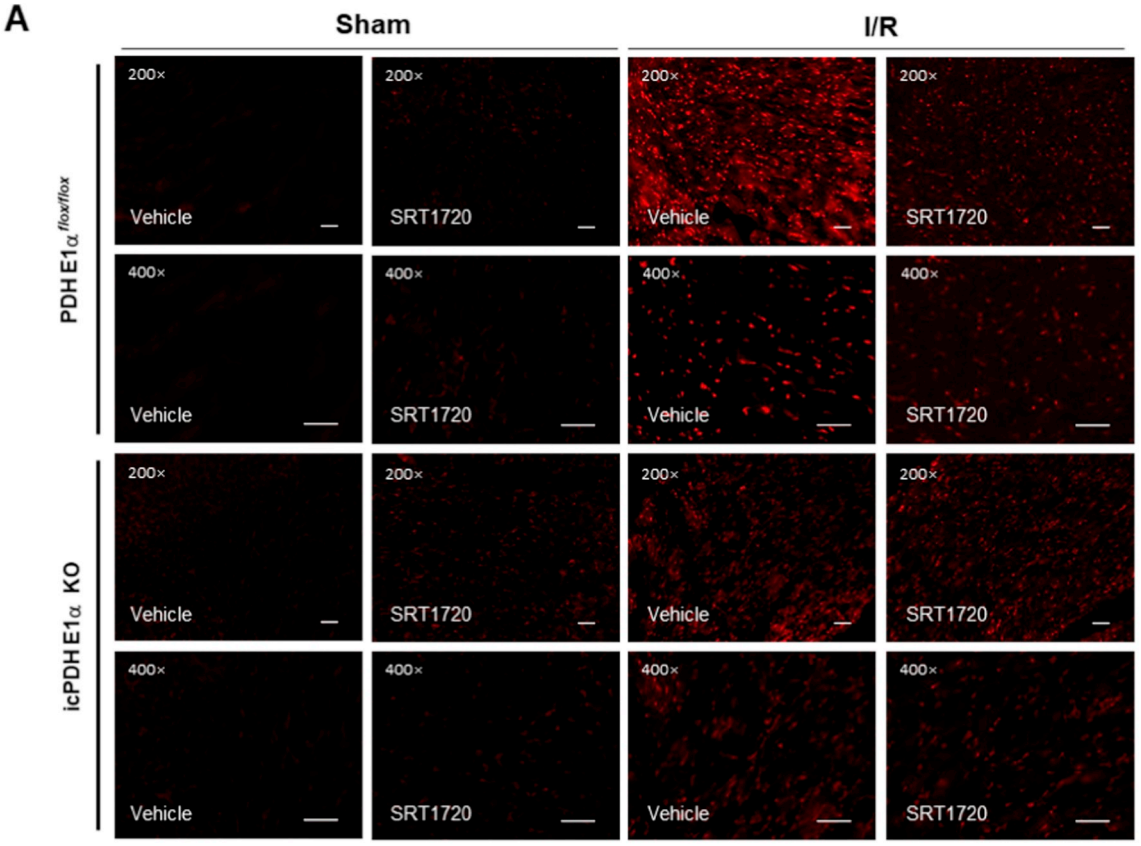

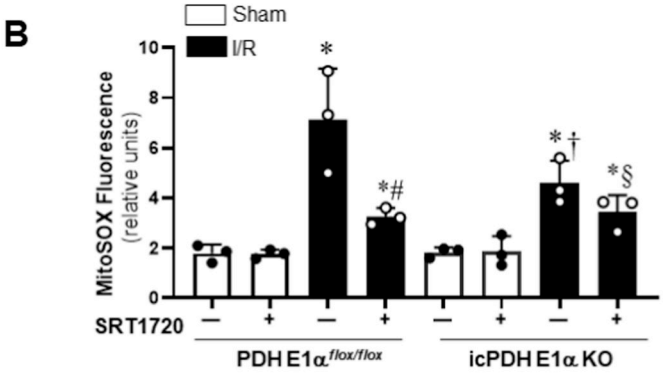

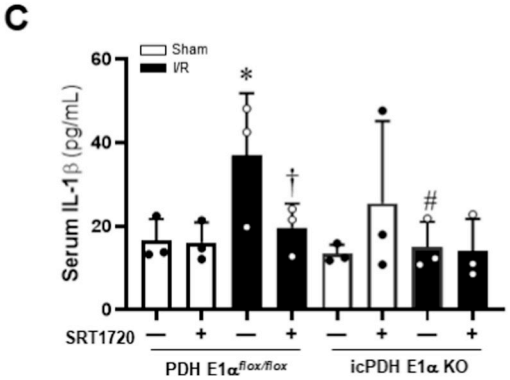

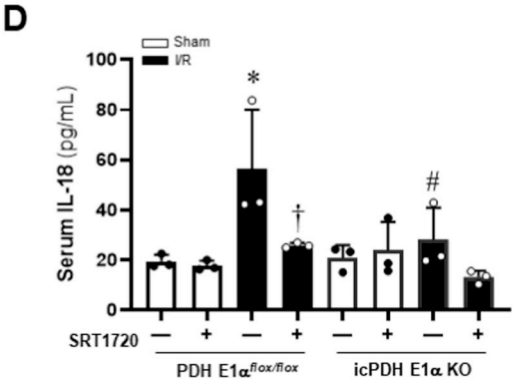

(caption on next page)

Fig. 6. Effects of SRT1720 treatments on ROS and NLRP3 inflammasome activation in response to I/R stress in PDH E1α$^{flox/flox}$ and icPDH E1α KO hearts. (A) The representative images of mitochondrial superoxide production (MitoSOX, red fluorescence) of PDH E1α$^{flox/flox}$ and icPDH E1α KO hearts under sham operations and I/R with or without SRT1720 treatments. (B) Quantitative analysis of MitoSOX production. N = 3 mice/each group, *p < 0.05 *vs.* Sham with vehicle, respectively; #p < 0.05 *vs.* I/R with vehicle in PDH E1α$^{flox/flox}$; †p < 0.05 *vs.* I/R with vehicle in PDH E1α$^{flox/flox}$; §p < 0.05 *vs.* I/R with SRT1720 in PDH E1α$^{flox/flox}$. (C) The serum IL-1β levels in PDH E1α$^{flox/flox}$ and icPDH E1α KO mice under sham and I/R with or without SRT1720 treatments. N = 3 mice/group, *p < 0.05 *vs.* Sham with vehicle in PDH E1α$^{flox/flox}$; †p < 0.05 *vs.* I/R with vehicle in PDH E1α$^{flox/flox}$; #p < 0.05 *vs.* I/R with vehicle in PDH E1α$^{flox/flox}$. (D) The serum IL-18 levels in PDH E1α$^{flox/flox}$ and icPDH E1α KO mice under sham and I/R with or without SRT1720 treatments. n = 3/group, *p < 0.05 *vs.* Sham with vehicle in PDH E1α$^{flox/flox}$; †p < 0.05 *vs.* I/R with vehicle in PDH E1α$^{flox/flox}$; #p < 0.05 *vs.* I/R with vehicle in PDH E1α$^{flox/flox}$. (E) Upper left: the immunoblotting to show PDH, NLRP3, PTEN, PI3K, Akt, AMPK, ACC and CPT-1 signaling response in PDH E1α$^{flox/flox}$ and icPDH E1α KO hearts under sham and I/R with or without SRT1720 treatments. Right and lower: quantitative analysis of NLRP3, PTEN, Akt, AMPK, ACC and CPT1 levels in PDH E1α$^{flox/flox}$ and icPDH E1α KO hearts under sham and I/R with or without SRT1720 treatments. N = 3 mice/each group, *p < 0.05 *vs.* Sham with vehicle in PDH E1α$^{flox/flox}$; †p < 0.05 *vs.* I/R with vehicle in PDH E1α$^{flox/flox}$; #p < 0.05 *vs.* I/R with vehicle in PDH E1α$^{flox/flox}$; §p < 0.05 *vs.* I/R + SRT1720 in PDH E1α$^{flox/flox}$. (For interpretation of the references to colour in this figure legend, the reader is referred to the Web version of this article.)

decreased phosphorylation of PDH (inactive form of PDH) during I/R, representing that I/R triggered activation of PDH and glucose oxidative metabolism, while SIRT1 activation by SRT1720 administration significantly inhibited PDH activity, resulting in the inhibition of NLRP3 inflammasome activation.

ROS generation has been identified as an important mechanism by which NLRP3 inflammasome is activated, and NLRP3 activation was blocked by ROS scavengers [51]. In the present study, we found that the

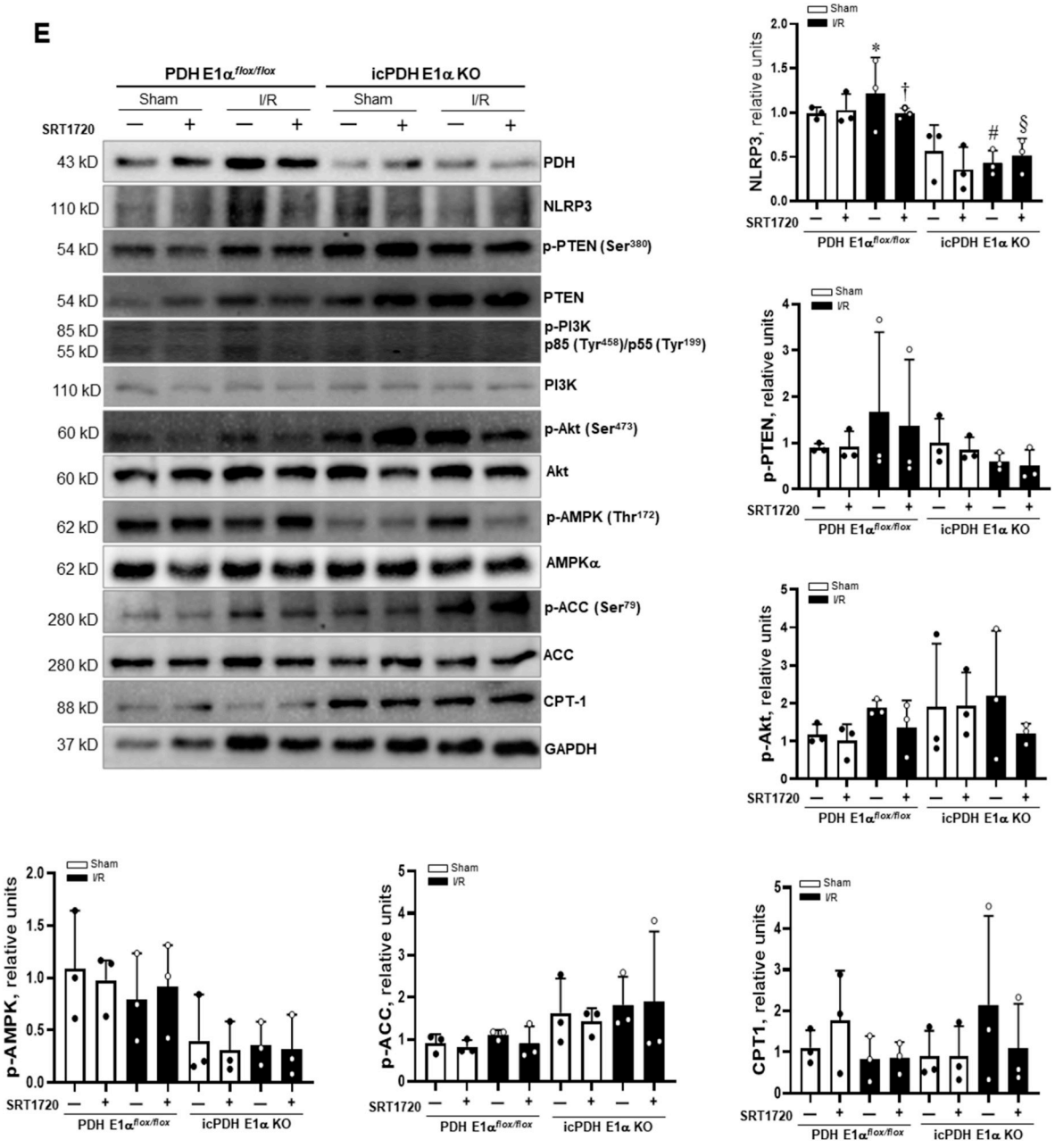

Fig. 6. (*continued*)

activation of NLRP3 inflammasome significantly increased in a ROS-dependent manner to induce pyroptotic cell death during myocardial I/R injury. SIRT1 agonist SRT1720 suppressed the activation of the NLRP3 inflammasome and reduced the secretion of IL-1β and IL-18, along with a reduction in ROS generation. Like the glucose metabolism of tumor cells, there is dynamic change in myocardial energy metabolism during the ischemia-reperfusion period. It is well known that metabolism shifts from aerobic oxidation to glycolysis under ischemia stress. According to our results, glucose oxidation became active at 6 h of reperfusion according to our results, providing ATP for cardiomyocytes. However, excessive glucose oxidative metabolism was followed by more ROS generation and reduced NAPDH, inducing oxidative damage. Moreover, SIRT1 activation reversed the excessive glucose oxidative metabolism, attenuated ROS generation and NLRP3 inflammasome-induced pyroptosis to protect the heart against I/R injury. Taken together, we believe that SIRT1 can balance the metabolic change, shift towards the normal myocardial energy metabolism to inhibit NLRP3 inflammasome against I/R injury.

5. Conclusion

This work defined a role of SIRT1 in NLRP3 inflammasome activation during myocardial ischemia and reperfusion. Pyruvate dehydrogenase mediates the activation of NLRP3 inflammasome in response to ischemia and reperfusion stress. Facing the challenge of protection for myocardial ischemic insults caused by ischemia and reperfusion injury, SIRT1 signaling shows a therapeutic potential not only in myocardial energy metabolism, but also in the inhibition of NLRP3 inflammasome.

Author contributions

J. Li conceived and designed the study, participated in the revision and final approval of the manuscript. Y. Han and W. Sun participated in the study design, data collection, and in the writing of the draft manuscript. D. Ren, J. Zhang, Z. He,J. Fedorova, X. Sun and F. Han participated in the partial data collection. All authors read and approved the final manuscript.

Funds

The present study was partly supported by the State Administration of Foreign Experts Affairs of China (P182011020). American Diabetes Association (ADA) 1-17-IBS-296. Excellent youth project of the Fourth Affiliated Hospital of Harbin Medical University No. HYDSYYXQN202007.

Declaration of competing interest

The authors declare that they have no conflict of interest.

Appendix A. Supplementary data

Supplementary data to this article can be found online at https://doi.org/10.1016/j.redox.2020.101538.

References

[1] E.J. Benjamin, M.J. Blaha, S.E. Chiuve, M. Cushman, S.R. Das, R. Deo, J. Floyd, M. Fornage, C. Gillespie, C. Isasi, Heart disease and stroke statistics-2017 update: a report from the American Heart Association, Circulation 135 (10) (2017) e146–e603.
[2] P.Z. Gerczuk, R.A. Kloner, An update on cardioprotection: a review of the latest adjunctive therapies to limit myocardial infarction size in clinical trials, J. Am. Coll. Cardiol. 59 (11) (2012) 969–978.
[3] A.C.O.E. Physicians, P.T. O'Gara, F.G. Kushner, D.D. Ascheim, C.D. Jr, M.K. Chung, J.A. de Lemos, S.M. Ettinger, J.C. Fang, ACCF/AHA guideline for the management of ST-elevation myocardial infarction: a rep dnnort of the American College of Cardiology, Found./Am. Heart Assoc. Task Force Pract. Guidel. 61 (4) (2013) e78–e140 2013.
[4] D.J. Hausenloy, D.M. Yellon, Targeting myocardial reperfusion injury — the search continues, N. Engl. J. Med. 373 (11) (2015) 1073–1075.
[5] D.J. Hausenloy, D.M. Yellon, Time to take myocardial reperfusion injury seriously, N. Engl. J. Med. 359 (5) (2008) 518–520.
[6] M. Neri, I. Riezzo, N. Pascale, C. Pomara, E. Turillazzi, Ischemia/reperfusion injury following acute myocardial infarction: a critical issue for clinicians and forensic pathologists, Mediat. Inflamm. 2017 (2017) 7018393.
[7] P. Pagliaro, F. Moro, F. Tullio, M.-G. Perrelli, C. Penna, Cardioprotective pathways during reperfusion: focus on redox signaling and other modalities of cell signaling, Antioxidants Redox Signal. 14 (5) (2011) 833–850.
[8] Piper, A fresh look at reperfusion injury, Cardiovasc. Res. 38 (2) (1998) 291–300.
[9] T. Reffelmann, R.A. Kloner, The no-reflow phenomenon: a basic mechanism of myocardial ischemia and reperfusion, Basic Res. Cardiol. 101 (5) (2006) 359–372.
[10] S. Verma, P.W.M. Fedak, R.D. Weisel, J. Butany, V. Rao, A. Maitland, R.K. Li, B. Dhillon, T.M. Yau, Fund. Reperfusion Inj. Clin. Cardiol. 105 (20) (2002) 2332–2336.
[11] C.P. Baines, How and when do myocytes die during ischemia and reperfusion: the late phase, J. Cardiovasc. Pharmacol. Therapeut. 16 (3–4) (2011) 239–243.
[12] Eugene Braunwald, The war against heart failure: the Lancet lecture, Lancet 385 (9970) (2015) 812–824.
[13] Z.Q. Zhao, Oxidative stress-elicited myocardial apoptosis during reperfusion, Curr. Opin. Pharmacol. 4 (2) (2004) 159–165.
[14] Y. Liu, K. Lian, L. Zhang, R. Wang, F. Yi, G. Chao, TXNIP mediates NLRP3 inflammasome activation in cardiac microvascular endothelial cells as a novel mechanism in myocardial ischemia/reperfusion injury, Basic Res. Cardiol. 109 (5) (2014) 415.
[15] H. Guo, J.B. Callaway, J.P.-Y. Ting, Inflammasomes: mechanism of action, role in disease, and therapeutics, Nat. Med. 21 (7) (2015) 677–687.
[16] F. Martinon, K. Burns, J. Tschopp, The inflammasome: a molecular platform triggering activation of inflammatory caspases and processing of proIL-beta, Mol. Cell 10 (2) (2002) 417–426.
[17] L. Wang, G.A. Manji, J.M. Grenier, A. Al-Garawi, S. Merriam, J.M. Lora, B.J. Geddes, M. Briskin, P.S. DiStefano, J. Bertin, PYPAF7, a novel PYRIN-containing apaf1-like protein that regulates activation of NF-kappa B and caspase-1-dependent cytokine processing, J. Biol. Chem. 277 (33) (2002) 29874–29880.
[18] C.A. Dinarello, Immunological and inflammatory functions of the interleukin-1 family, Annu. Rev. Immunol. 27 (1) (2009) 519–550.
[19] S.L. Fink, B.T. Cookson, Caspase-1-dependent pore formation during pyroptosis leads to osmotic lysis of infected host macrophages, Cell Microbiol. 8 (11) (2006) 1812–1825.
[20] O. Sandanger, T. Ranheim, L.E. Vinge, M. Bliksoen, K. Alfsnes, A.V. Finsen, C.P. Dahl, E.T. Askevold, G. Florholmen, G. Christensen, The NLRP3 inflammasome is up-regulated in cardiac fibroblasts and mediates myocardial ischaemia-reperfusion injury, Cardiovasc. Res. 99 (1) (2013) 164–174.
[21] Masafumi Takahashi, NLRP3 inflammasome as a novel player in myocardial infarction, Int. Heart J. 55 (2) (2014) 101–105.
[22] S. Toldo, A.G. Mauro, Z. Cutter, A. Abbate, Inflammasome, pyroptosis, and cytokines in myocardial ischemia-reperfusion injury, Am. J. Physiol. Heart Circ. Physiol. 315 (6) (2018) H1553–H1568.
[23] M.M. Hughes, L.A.J. O'Neill, Metabolic regulation of NLRP3, Immunol. Rev. 281 (1) (2018) 88–98.
[24] H. Wen, D. Gris, Y. Lei, S. Jha, L. Zhang, M.T.-H. Huang, W.J. Brickey, J.P.-Y. Ting, Fatty acid–induced NLRP3-ASC inflammasome activation interferes with insulin signaling, Nat. Immunol. 12 (5) (2011) 408–415.
[25] E.L. Goldberg, J.L. Asher, R.D. Molony, A.C. Shaw, C.J. Zeiss, C. Wang, L.A. Morozova-Roche, R.I. Herzog, A. Iwasaki, V.D. Dixit, β-Hydroxybutyrate deactivates neutrophil NLRP3 inflammasome to relieve gout flares, Cell Rep. 18 (9) (2017) 2077–2087.
[26] Y.-H. Youm, K.Y. Nguyen, R.W. Grant, E.L. Goldberg, M. Bodogai, D. Kim, D. D'Agostino, N. Planavsky, C. Lupfer, T.D. Kanneganti, The ketone metabolite β-hydroxybutyrate blocks NLRP3 inflammasome–mediated inflammatory disease, Nat. Med. 21 (3) (2015) 263–269.
[27] A.J. Wolf, C.N. Reyes, W. Liang, C. Becker, K. Shimada, M.L. Wheeler, H.C. Cho, N.I. Popescu, K.M. Coggeshall, M. Arditi, D.M. Underhill, Hexokinase is an innate immune receptor for the detection of bacterial peptidoglycan, Cell 166 (3) (2016) 624–636.
[28] J.-S. Moon, S. Hisata, M.-A. Park, G.M. DeNicola, S.W. Ryter, K. Nakahira, A.M.K. Choi, mTORC1-Induced HK1-dependent glycolysis regulates NLRP3 inflammasome activation, Cell Rep. 12 (1) (2015) 102–115.
[29] C.P. Hsu, I. Odewale, R.R. Alcendor, J. Sadoshima, Sirt1 protects the heart from aging and stress, Biol. Chem. 389 (3) (2008) 221–231.
[30] S. Rane, M. He, D. Sayed, H. Vashistha, A. Malhotra, J. Sadoshima, D.E. Vatner, S.F. Vatner, M. Abdellatif, Downregulation of MiR-199a derepresses hypoxia-inducible factor-1α and sirtuin 1 and recapitulates hypoxia preconditioning in, Cardiac Myocytes 104 (7) (2009) 879–886.
[31] K. Shinmura, K. Tamaki, R. Bolli, Impact of 6-mo caloric restriction on myocardial ischemic tolerance: possible involvement of nitric oxide-dependent increase in nuclear Sirt1, Am. J. Physiol. Heart Circ. Physiol. 295 (6) (2008) H2348–H2355.
[32] C. Tong, A. Morrison, S. Mattison, S. Qian, M. Bryniarski, B. Rankin, J. Wang, D.P. Thomas, J. Li, Impaired SIRT1 nucleocytoplasmic shuttling in the senescent heart during ischemic stress, Faseb. J. 27 (11) (2013) 4332–4342.
[33] L. Wang, N. Quan, W. Sun, X. Chen, C. Cates, T. Rousselle, X. Zhou, X. Zhao, J. Li, Cardiomyocyte specific deletion of Sirt1 gene sensitizes myocardium to ischemia

and reperfusion injury, Cardiovasc. Res. 114 (6) (2018) 805–821.
[34] R. Gao, Z. Ma, Y. Hu, J. Chen, S. Shetty, J. Fu, Sirt1 restrains lung inflammasome activation in a murine model of sepsis, Am. J. Physiol. Lung Cell Mol. Physiol. 308 (8) (2015) L847–L853.
[35] Y. Li, X. Yang, Y. He, W. Wang, J. Zhang, W. Zhang, T. Jing, B. Wang, R. Lin, Negative regulation of NLRP3 inflammasome by SIRT1 in vascular endothelial cells, Immunobiology 222 (3) (2017) 552–561.
[36] M. Chen, T. Wang, Y. Shen, D. Xu, X. Li, J. An, J. Dong, D. Li, F. Wen, L. Chen, Knockout of RAGE ameliorates mainstream cigarette smoke-induced airway inflammation in mice, Int. Immunopharm. 50 (2017) 230–235.
[37] M.T. Johnson, S. Mahmood, S.L. Hyatt, H.S. Yang, M.S. Patel, Inactivation of the murine pyruvate dehydrogenase (Pdha1) gene and its effect on early embryonic development, Mol. Genet. Metabol. 74 (3) (2001) 293–302.
[38] C. Tong, A. Morrison, S. Mattison, S. Qian, M. Bryniarski, B. Rankin, J. Wang, D.P. Thomas, J. Li, Impaired SIRT1 nucleocytoplasmic shuttling in the senescent heart during ischemic stress, Faseb. J. 27 (11) (2013) 4332–4342.
[39] Q. Lu, J. Liu, X. Li, X. Sun, J. Zhang, D. Ren, N. Tong, J. Li, Empagliflozin attenuates ischemia and reperfusion injury through LKB1/AMPK signaling pathway, Mol. Cell. Endocrinol. 501 (2020) 110642.
[40] S. Toldo, E. Mezzaroma, A.G. Mauro, F.N. Salloum, A.V.E. Abbate, The inflammasome in myocardial injury and cardiac remodeling, Antioxidants Redox Signal. 22 (13) (2015) 1146–1161.
[41] J.N. Cohn, R. Ferrari, N. Sharpe, Cardiac remodeling-concepts and clinical implications: a consensus paper from an international forum on cardiac remodeling. Behalf of an international forum on cardiac remodeling, J. Am. Coll. Cardiol. 35 (3) (2000) 569–582.
[42] N.G. Frangogiannis, C.W. Smith, M.L. Entman, The inflammatory response in myocardia; infarction, Cardiovasc. Res. 53 (1) (2002) 31–47.
[43] I.M. Seropian, S. Toldo, B.W. Van Tassell, A. Abbate, Anti-inflammatory strategies for ventricular remodeling following ST-segment elevation acute myocardial infarction, J. Am. Coll. Cardiol. 63 (16) (2014) 1593–1603.
[44] S. Toldo, C. Marchetti, A.G. Mauro, J. Chojnacki, E. Mezzaroma, S. Carbone, S. Zhang, B. Van Tassell, F.N. Salloum, A. Abbate, Inhibition of the NLRP3 inflammasome limits the inflammatory injury following myocardial ischemia–reperfusion in the mouse, Int. J. Cardiol. 209 (2016) 215–220.
[45] M. Kawaguchi, M. Takahashi, T. Hata, Y. Kashima, F. Usui, H. Morimoto, A. Izawa, Y. Takahashi, J. Masumoto, J. Koyama, Inflammasome activation of cardiac fibroblasts is essential for myocardial ischemia/reperfusion injury, Circulation 123 (6) (2011) 594–604.
[46] Y. He, H. Hara, G. Núnez, Mechanism and regulation of NLRP3 inflammasome activation, Trends Biochem. Sci. 41 (12) (2016) 1012–1021.
[47] C. Dempsey, A.R. Araiz, K.J. Bryson, O. Finucane, C. Larkin, E.L. Mills, A.A.B. Robertson, M.A. Cooper, L.A.J. O'Neill, M.A. Lynch, Inhibiting the NLRP3 inflammasome with MCC950 promotes non-phlogistic clearance of amyloid-β and cognitive function in APP/PS1 mice, Brain Behav. Immun. 61 (2017) 306–316.
[48] D. Jiang, S. Chen, R. Sun, X. Zhang, D. Wang, The NLRP3 inflammasome: role in metabolic disorders and regulation by metabolic pathways, Canc. Lett. 419 (2018) 8–19.
[49] S.S. Iyer, Q. He, J.R. Janczy, E.I. Elliott, Z. Zhong, A.K. Olivier, J.J. Sadler, V. Knepper-Adrian, R. Han, L. Qiao, S.C. Eisenbarth, W.M. Nauseef, S.L. Cassel, F.S. Sutterwala, Mitochondrial cardiolipin is required for Nlrp3 inflammasome activation, Immunity 39 (2) (2013) 311–323.
[50] A. Frank, M. Bonney, S. Bonney, L. Weitzel, M. Koeppen, T. Eckle, Myocardial ischemia reperfusion injury: from basic science to clinical bedside, Semin. CardioThorac. Vasc. Anesth. 16 (3) (2012) 123–132.
[51] C.M. Yang, I.-T. Lee, R.-C. Hsu, P.-L. Chi, L.-D. Hsiao, NADPH oxidase/ROS-dependent PYK2 activation is involved in TNF-α-induced matrix metalloproteinase-9 expression in rat heart-derived H9c2 cells, Toxicol. Appl. Pharmacol. 272 (2) (2013) 431–442.